A NEW METHOD FOR BROADENING BANDWIDTHS OF CIRCULAR POLARIZED MICROSTRIP ANTENNAS BY USING DGS & PARASITIC SPLIT-RING RESONATORS

Zhaobin Deng, Wen Jiang, Shuxi Gong[*], Yunxue Xu, and Yang Zhang

National Laboratory of Science and Technology on Antennas and Microwaves, Xidian University, Xi'an 710071, P. R. China

Abstract—A new method for broadening the impedance and the axialratio (AR) bandwidths of circular polarized microstrip antennas (CPMAs) is proposed. It has improved the bandwidths of a reference antenna greatly without enlarging the antenna size or deteriorating circular polarized radiation characteristics by placing four sequentially rotated parasitic split-ring resonators (SRRs) around the patch of the reference antenna and embedding four defeated ground structure (DGS) elements on the ground plane. Improvements of 51.3% and 49.8% in the impedance and the axial-ratio bandwidths of the antenna are achieved in simulation, respectively. The simulated $-10\,\text{dB}$ impedance and $3\,\text{dB}$ axial-ratio bandwidths of the antenna have been improved from $101.1\,\text{MHz}$ (4.12%) to $153.0\,\text{MHz}$ (6.26%) and from $25.1\,\text{MHz}$ (1.02%) to $37.6\,\text{MHz}$ (1.54%).

1. INTRODUCTION

Recently, many researches have been conducted on circular polarized microstrip antennas (CPMAs), since they are extensively used in wireless communication systems due to their advantages such as low profile, light weight and conformal to the mounting structure. Moreover, communication systems with circular polarized (CP) antennas can reduce antenna orientation angle constraints between the transmitter and the receiver and suppress multipath reflections [1–5]. However, the bandwidth of CPMAs is narrow in most occasions [6, 7], causing severe limitations for practical applications.

* Corresponding author: Shuxi Gong (shxgong@xidian.edu.cn).

Many methods have been proposed to broaden the bandwidths of single-fed CMPAs. A thick substrate or a large ground plane is often used [8]. Slotting in the antenna patch is a widely used method. Cutting a U-slot, equal and unequal parallel slots on the patch to obtain a wide axial-ratio (AR) bandwidth are reported in [9, 10], respectively. Slotting in the ground plane is another way to achieve wide bandwidths. A corners truncated microstrip antenna with a group of four bent slots in the ground plane is put forward in [11]. By embedding the slots, the bandwidths of the antenna are enhanced. Adding external structures is also effective in bandwidth broadening. A metamaterial reflective surface as a superstrate for a single-feed CPMA is reported in [12], which may enhance the bandwidths greatly. An electromagnetic band gap (EBG) structure is employed in [13] for higher gain and wider bandwidths due to the reduction of surface waves. In [14], a cross slot on the patch with four nonlinear diodes can enhance the AR bandwidth due to the nonlinear coupling between resonant modes through the diodes. In [15], a slotted patch with four sets of arms at the diagonal corners is divided into two parts, an excited part with a short wall and a coupling part. Two modes which resonate at nearby frequencies can be excited and a broad bandwidth is obtained. Besides, in [16], a single probe-fed microstrip patch antenna with truncated corners is placed at the center of an antenna array as the driven antenna and is gapped coupled to the remaining parasitic elements. Wider impedance and axial-ratio bandwidths are observed.

Wide bandwidths are achieved by using the methods which are mentioned above. However, these methods may have deficiencies such as: deteriorating circular polarized radiation characteristics [9–11], being sensitive to antenna structure parameters [13–15] and requiring a large antenna dimension [12, 16]. In this paper, a new method for broadening the impedance and the AR bandwidths of CPMAs is proposed. By adding four sequentially rotated parasitic split-ring resonators (SRRs) and four defeated ground structure (DGS) elements, the bandwidths of a reference antenna are improved greatly. Since the parasitic SRRs are placed around the patch of the reference antenna, the patch is not modified and the circular polarized radiation characteristics are not influenced. As the SRRs and DGS elements are simple structures, the antenna performances are not sensitive to the structure parameters. A large antenna dimension is not required due to no periodic structures are employed in this design. In general, deficiencies are overcome in this design while impedance and AR bandwidths are improved.

The performance of the design in this paper comparing with the state-of-the-art literature reference [13] is shown in Table 1. The

Table 1. The performance of the proposed design comparing with Reference [13].

Design	Overall Antenna Volume (λ_0^3)	f_c (MHz)	$-10\,\text{dB}$ Impedance BW (MHz)	$3\,\text{dB AR}$ BW (MHz)
Ref. [13]	$0.42 \times 0.42 \times 0.01$	1575	22	9
Proposed	$0.29 \times 0.29 \times 0.026$	2450	153.0	37.6

Design	Gain (dB)	Increase in impedance BW over Ref. Ant (%)	Increase in AR BW over Ref. Ant (%)	Increase in Gain over Ref. Ant (%)
Ref. [13]	7.0	0	60	21
Proposed	4.3	51.3	49.8	0

design in [13] has improved the AR bandwidth of a reference single-feed CPMAs without requiring a large antenna dimension or deteriorating circular polarized radiation characteristics, which is similar with the design proposed in this paper. As shown in Table 1, the design in [13] provides more increase in AR bandwidth and gain with a lower profile, while its limitations are that the structure based on the 2nd iteration of the fractal requires higher manufacture accuracy and no increase in S_{11} bandwidth is obtained. As for the design in this paper, the impedance and AR bandwidths are improved simultaneously with a smaller antenna area and lower manufacture accuracy. It is shown that the design in this paper have more practical significance in modern wireless communication applications.

2. ANTENNA STRUCTURE AND DESIGN

2.1. Antenna Structure

The reference antenna is a traditional diagonal corners truncated circular polarized microstrip antenna which is printed on a square substrate with a thickness of 3.18 mm and a relative dielectric constant of 10.92, as depicted in Figure 1. The size of the antenna is $35 \times 35 \times 3.18\,\text{mm}^3$, around $0.29\lambda_0 \times 0.29\lambda_0 \times 0.026\lambda_0$ in terms of the resonance frequency, 2.45 GHz. The principal polarization of the reference antenna is right-hand circular polarization (RHCP). A 50-Ω coaxial probe-feeding is utilized. As for the proposed antenna, the configuration is shown in Figures 2(a)–(c). Four sequentially rotated parasitic split-ring resonators (SRRs) are placed around the patch
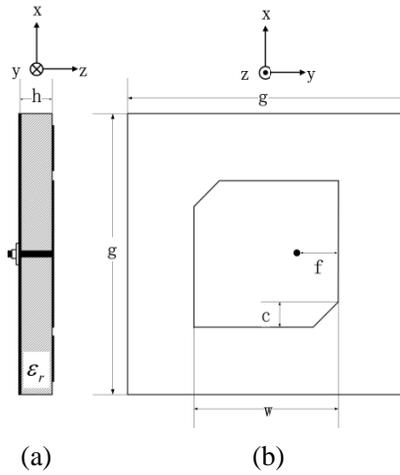
Figure 1. The Configuration of the reference antenna. (a) Side view. (b) Top view.
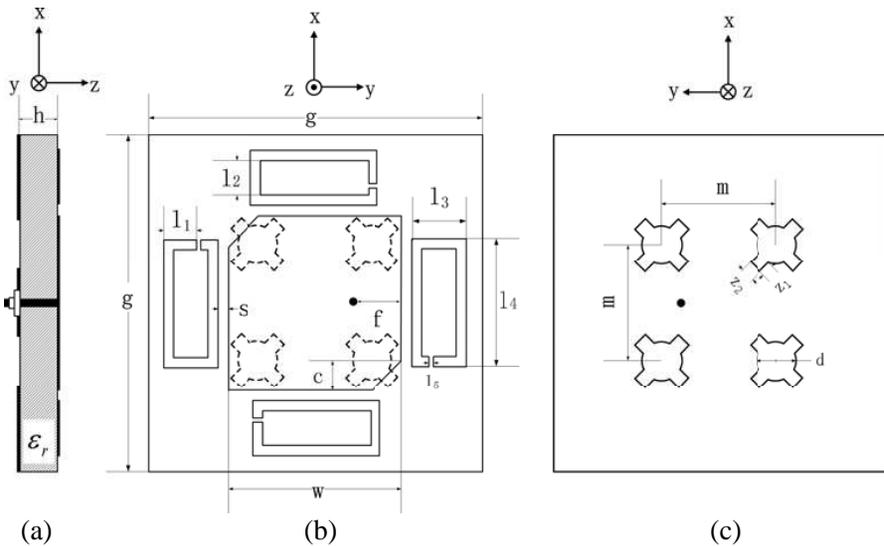
Figure 2. Proposed antenna configuration. (a) Side view. (b) Top view. (c) Bottom view.

of the reference antenna with a distance of s. Four symmetrically arranged defected ground structure (DGS) elements are etched on the ground plane of the reference antenna. The dimensions of the reference and the proposed antennas are listed in Tables 2 and 3 in details.

Table 2. Dimensions of the reference antenna.

Dimension	g	w	c	f	h
(mm)	35	17	2.1	3.1	3.18

Table 3. Dimensions of the proposed antenna.

Dimension	g	w	c	f	s	l_1	l_2	l_3
(mm)	35	16.7	3.3	4.2	1.2	4	4	5.4
Dimension	l_4	l_5	h	m	d	z_1	z_2	
(mm)	13.5	0.5	3.18	12.2	4.2	1.2	1.5	

2.2. Parasitic Split-ring Resonators Design

As well known, parasitic patches have been used for improving bandwidths of microstrip antennas for decades [16–18]. However, due to the parasitic patches are $\lambda_m/2$ resonators (λ_m is the guided wavelength for microstrip transmission line at central frequency), the overall sizes of the antennas are enlarged. As another shape of parasitic element, parasitic split-ring resonators have been used in loop antennas [19] and dipole antennas [20], achieving a wide bandwidth without changing the antenna size. Since $l_c = n\lambda_g/2$ [20] (l_c is the circumference of the SRRs, and λ_g is the guided wavelength at central frequency, $n \in N$), the value of l_c changes with the variation of n when λ_g is determined.

As for the proposed antenna, the value of n is chosen as 2 through simulation experiments. In simulation, the increases in bandwidths are not obvious when $n = 1$, and the SRRs may occupy a large area when $n = 3$. Current-vector distribution on the patch and the loops at the central frequency 2.446 GHz is depicted in Figure 3. As shown in Figure 3, resonating at the nearby central frequency, SRRs are gap-coupling from the radiating edges of the patch. A difference in the phases of the currents on the patch and the resonators can be observed because of different resonance frequencies. At $0°$, the currents on two opposite resonators reach the maximum value and flow in the x direction and decrease to zero at $90°$. While at $90°$, the currents on the other resonators maximize and flow in the negative y direction. Currents flow in the opposite direction at $180°$ and $270°$. It is clear that orthogonal resonators radiate two orthogonal linear polarized electric components with equal amplitudes modes and $90°$ phase difference. In this way, four parasitic resonators can be considered as a circular polarized radiator. By resonating at the nearby frequency of the patch,
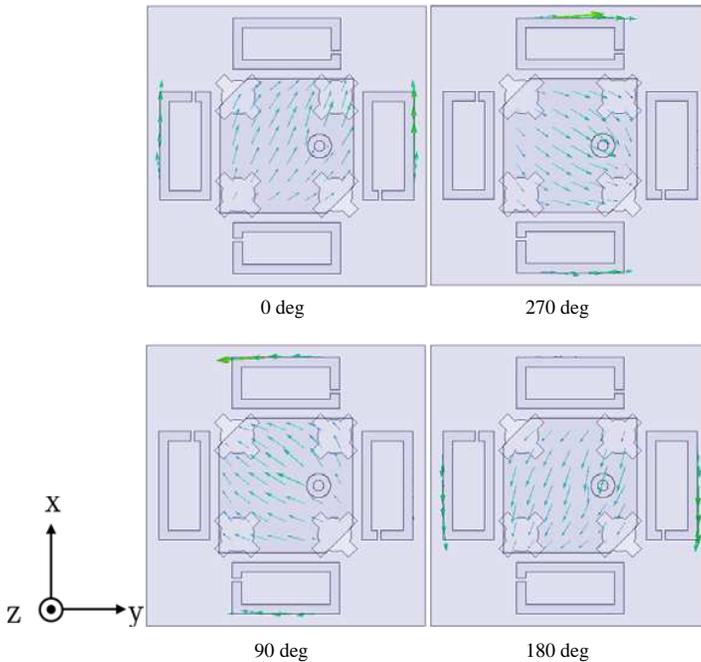
Figure 3. The current-vector distribution on the patch and the loops at 2.446 GHz.

the impedance and 3 dB axial-ratio bandwidths of the antenna are improved.

2.3. Defected Ground Structure Elements Design

Embedding suitable slots in the finite ground plane can cause meandering of the excited surface current paths, which would reduce the resonance frequency and the quality factor of the antenna effectively and obtain wider impedance and AR bandwidths [12, 21].

In this paper, as shown in Figure 2, four DGS elements which consist of a circle and four stubs are embedded in the ground plane. Elements are placed below the corners of the patch to keep a proper distance from the feed port. Current-vector distribution on the ground plane at 2.446 GHz is depicted in Figure 4. From Figure 4, at 0°, currents flow in the x direction. While at 90°, currents flow in the negative y direction. Currents surround the stubs follow an orthogonal path. Similarly, at the 180° and 270°, both currents are in opposite directions. It can be observed that the current path on the ground
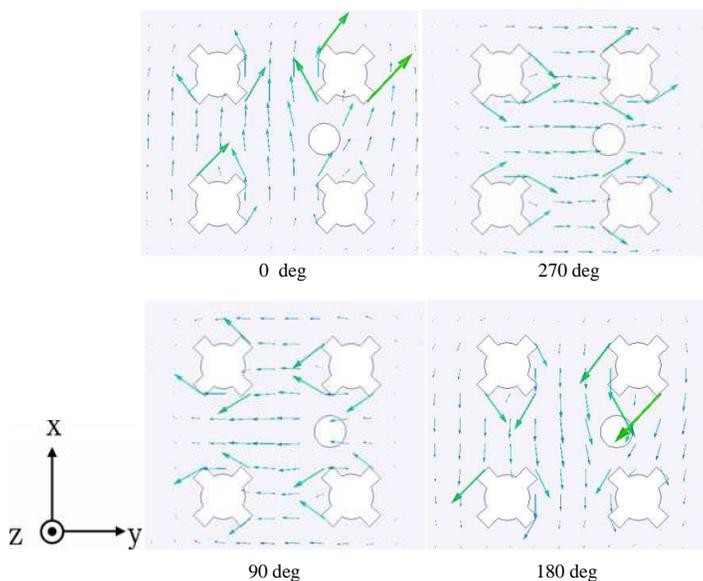
Figure 4. The current-vector distribution on the ground plane at 2.446 GHz.

plane is meandered obviously, which leads to a reduction in the quality factor and wider bandwidths.

The distance between nearby elements, m, and the diameter of the circle, d, influence the current path on the ground plane and determine the resonance frequency and the bandwidth. The length and the width of the stubs, z_1 and z_2, adjust the orthogonal current path slightly. Compared to the slots, circles occupy more area and have a longer border, which can bend the current path further. Stubs added to the circle are designed for lengthening the current path and guiding currents around the circle to follow an orthogonal path to improve circular polarized radiation characteristics.

3. EXPERIMENTAL VERIFICATION

In this paper, the simulations are implemented using the analysis software Ansoft HFSS 13. CP performances with different structures in simulation are listed in Table 4. Photos of the prototypes of the reference and the proposed antennas are shown in Figure 5. A comparison on the simulated and the measured return losses is shown in Figure 6. From Figure 6, both of the resonances are shifted toward lower frequencies and resonating at 2.39 GHz due to

Figure 5. The prototypes of the reference and the proposed antennas.

Table 4. Circular polarized performances with different structures.

Design	f_c	$-10\,\text{dB}$ impedance BW	$3\,\text{dB}$ AR BW	Increase in impedance/AR BW
	MHz	MHz	MHz	%
Ref. Ant	2454	101.1	25.1	0.0/0.0
Ref. Ant with DGS	2450	113.2	27.9	12.0/11.2
Ref. Ant with SRRs	2446	135.1	33.8	33.6/34.7
Ref. Ant with DGS & SRRs	2446	153.0	37.6	51.3/49.8
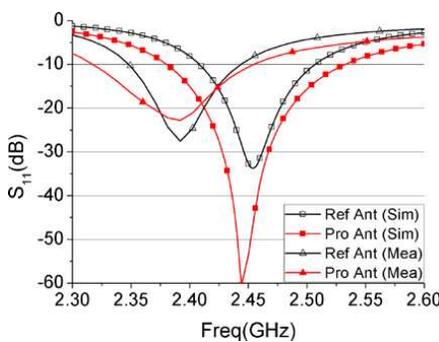
Figure 6. Simulated and measured S_{11}s.
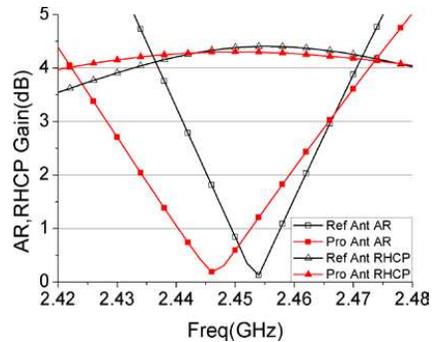
Figure 7. Axial-ratios and RHCP gains.

manufacture tolerances and the fluctuation in the dielectric constant of the substrate. The corresponding impedance bandwidths ($S_{11} \leq -10$ dB) of the reference and the proposed antennas are 101.1 MHz (4.12%) and 153.0 MHz (6.26%) in simulation, 96.0 MHz (4.02%) and 136.1 MHz (5.69%) in measurement. The simulated and the measured impedance bandwidths are improved by 51.3% and 41.6% upon the bandwidths of the reference antenna, respectively. Figure 7 depicts the simulated result of the ARs and RHCP gain of both antennas. The bandwidths for AR less than 3 dB of the reference and the proposed antennas are observed as 25.1 MHz (1.02%) and 37.6 MHz (1.53%). An

(a)   (b)
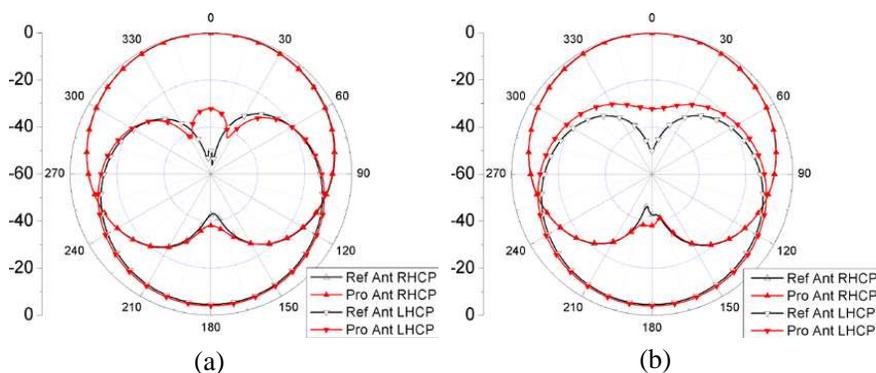
Figure 8. The normalized radiation patterns of the reference and the proposed antennas at their central frequencies 2.454 GHz and 2.446 GHz. (a) $\varphi = 0°$ plane. (b) $\varphi = 90°$ plane.

(a)   (b)
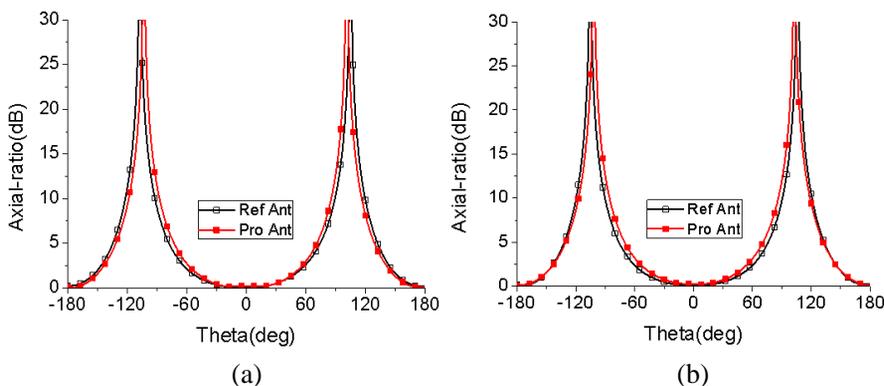
Figure 9. The patterns of AR of the reference antenna and the proposed antenna in elevation plane at their central frequencies 2.454 GHz and 2.446 GHz. (a) $\varphi = 0°$. (b) $\varphi = 90°$.

improvement of 49.8% in 3 dB axial-ratio bandwidths is achieved. The RHCP gains in the respective 3 dB AR bandwidth of the reference and the proposed antennas vary from 4.25 dB to 4.40 dB and from 4.11 dB to 4.30 dB. Radiation patterns of two principal planes $\varphi = 0°$ and $\varphi = 90°$ in simulation are depicted in Figure 8. From Figure 8, it is found that both antennas have similar radiation patterns. The back lobe of the proposed antenna is a little larger compared to the reference antenna. Because of embedding slots on the ground plane, the cross-polarization level increases from -50.07 dB to -32.35 dB, which is still acceptable. The patterns of AR of the reference antenna and the proposed antenna for $\varphi = 0°$ and $\varphi = 90°$ at their central frequencies are shown in Figures 9(a) and (b). The simulated ARs of the reference antenna and the proposed antenna are less than 3 dB in $\pm 60°$ coverage.

(a)   (b)

(c)
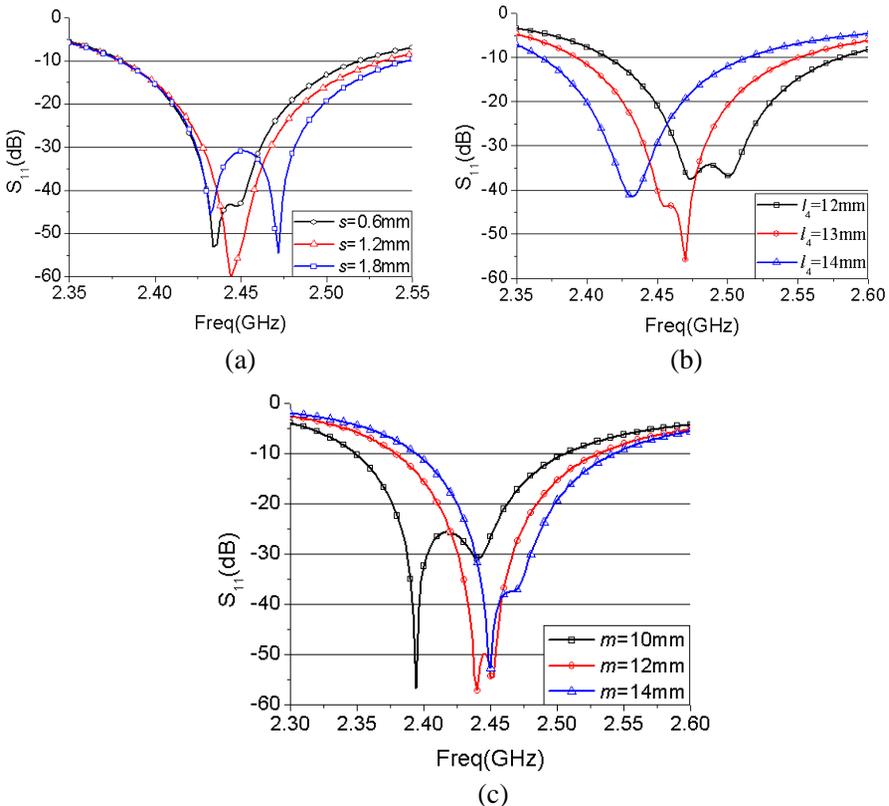
Figure 10. Simulated S_{11}s according to the variation of (a) s, (b) l_4, (c) m.

4. PARAMETRIC STUDIES

Figure 10(a) illustrates the simulated return losses versus gap s. The variation of s has an influence on the impedance of the antenna and leads to a change in the resonance frequencies of TM_{10} and TM_{01} modes. Although the widest bandwidth is generated when $s = 1.8\,\mathrm{mm}$, $s = 1.2\,\mathrm{mm}$ is selected to keep a minimum AR. To examine the effect of the circumference, the simulated return losses as a function of l_4 is plotted in Figure 10(b). The resonance of the antenna is shifted toward lower frequency significantly with increased l_4, since the resonance frequency is influenced by the circumstance of the SRRs. It can be observed that the bandwidth decreases slightly when $l_4 = 14\,\mathrm{mm}$. l_4 is selected as $13.5\,\mathrm{mm}$ in this paper as a compromise between a lower resonance frequency and a wider bandwidth. Figure 10(c) depicts the return losses when m is varied from $10\,\mathrm{mm}$ to $14\,\mathrm{mm}$. As shown in Figure 10(c), the current path on the ground plane is meandered severely when m is $10\,\mathrm{mm}$ and the resonance of the antenna is shifted toward lower frequency. When m is $14\,\mathrm{mm}$, the meandering of the path is little and the effect of the DGS elements is small. By considering manufacturing difficulty in welding the SMA connector, m is selected as $12.2\,\mathrm{mm}$.

5. CONCLUSION

A new method for broadening bandwidths of circular polarized microstrip antennas is proposed. Without changing the antenna size or deteriorating circular polarized performances, improvements of 51.3% and 49.8% in $-10\,\mathrm{dB}$ impedance and $3\,\mathrm{dB}$ axial-ratio bandwidths are achieved in simulation by placing four sequentially rotated parasitic split-ring resonators around the patch of the reference antenna and embedding four defeated ground structure elements on the ground plane. The $-10\,\mathrm{dB}$ impedance bandwidth is improved from $101.1\,\mathrm{MHz}$ (4.12%) to $153.0\,\mathrm{MHz}$ (6.26%) in simulation and from $96.0\,\mathrm{MHz}$ (4.02%) to $136.1\,\mathrm{MHz}$ (5.69%) in measurement. The $3\,\mathrm{dB}$ axial-ratio bandwidth in simulation is improved from $25.1\,\mathrm{MHz}$ (1.02%) to $37.6\,\mathrm{MHz}$ (1.53%). Simulated and measured results demonstrate that this method has improved the bandwidths of the reference antenna greatly without enlarging the antenna size or deteriorating circular polarized performances. Since this method is compact in size, simple in design and good in performance, it is suitable for other circular polarized microstrip antennas and has a practical significance in modern wireless communication applications.

ACKNOWLEDGMENT

REFERENCES

1. Tsai, C.-L., "A coplanar-strip dipole antenna for broad-band circular polarization operation," *Progress In Electromagnetics Research*, Vol. 121, 141–157, 2011.

2. Rezaeieh, S. A. and M. Kartal, "A new triple band circularly polarized square slot antenna design with crooked T and F-shape strips for wireless applications," *Progress In Electromagnetics Research*, Vol. 121, 1–18, 2011.

3. Joseph, R. and T. Fukusako, "Bandwidth enhancement of circularly polarized square slot antenna," *Progress In Electromagnetics Research B*, Vol. 29, 233–250, 2011.

4. Tsai, C.-L., "A coplanar-strip dipole antenna for broadband circular polarization operation," *Progress In Electromagnetics Research*, Vol. 121, 141–157, 2011.

5. Sze, J.-Y. and S.-P. Pan, "Design of broadband circularly polarized square slot antenna with a compact size," *Progress In Electromagnetics Research*, Vol. 120, 513–533, 2011.

6. Carver, K. and J. Mink, "Microstrip antenna technology," *IEEE Transactions on Antennas and Propagation*, Vol. 29, No. 1, 2–24, 1981.

7. Richards, W. and Y. Lo, "Design and theory of circularly polarized microstrip antennas," *Antennas and Propagation Society International Symposium*, Vol. 17, 117–120, 1979.

8. Tseng, C.-F. and C.-L. Huang, "Compact 2.5 GHz circularly polarized antenna using high permittivity substrate," *Asia-Pacific Conference Proceedings, Microwave Conference Proceedings*, Vol. 4, 2005.

9. Lam, K. Y., K.-M. Luk, K. F. Lee, H. Wong, and K. B. Ng, "Small circularly polarized U-slot wideband patch antenna," *IEEE Antennas and Wireless Propagation Letters*, Vol. 10, 87–90, 2011.

10. Khidre, A., K. F. Lee, F. Yang, and A. Eisherbeni, "Wideband circularly polarized E-shaped patch antenna for wireless applications," *IEEE Antennas and Propagation Magazine*, Vol. 52, No. 5, 219–229, 2010.

11. Chen, H.-D., "Compact circularly polarized microstrip antenna

with slotted ground plane," *Electronics Letters*, Vol. 38, No. 13, 616–617, 2002.

12. Chaimool, S., "Simultaneous gain and bandwidths enhancement of a single-feed circularly polarized microstrip patch antenna using a metamaterial reflective surface," *Progress In Electromagnetics Research B*, Vol. 22, 23–37, 2010.

13. Bao, X. L., G. Ruvio, M. J. Ammann, and M. John, "A novel GPS patch antenna on a fractal hi-impedance surface substrate," *IEEE Antennas and Wireless Propagation Letters*, Vol. 5, No. 1, 323–326, 2006.

14. Ushijima, Y., E. Nishiyama, and M. Aikawa, "Wide band switchable circularly polarized microstrip antenna using double-balanced multiplier," *IEEE Antennas and Propagation Society International Symposium*, 1–4, 2008.

15. Tang, X., H. Wong, Y. Long, Q. Xue, and K. L. Lau, "Circularly polarized shorted patch antenna on high permittivity substrate with wideband," *IEEE Transactions on Antennas and Propagation*, Vol. 60, No. 3, 1588–1592, 2012.

16. Chang, T. N. and J.-H. Jiang, "Enhance gain and bandwidth of circularly polarized microstrip patch antenna using gap-coupled method," *Progress In Electromagnetics Research*, Vol. 96, 127–139, 2009.

17. Kumar, G. and K. C. Gupta, "Nonradiating edges and four edges gap-coupled multiple resonator broad-band microstrip antennas," *IEEE Transactions on Antennas and Propagation*, Vol. 33, No. 2, 173–178, 1985.

18. Wood, C. and B. Sc, "Improved bandwidth of microstrip antennas using parasitic elements," *IEE Proceedings H — Microwaves, Optics and Antennas*, Vol. 127, 231–234, 1980.

19. Li, R., G. DeJean, J. Laskar, and M. M. Tentzeris, "Investigation of circularly polarized loop antennas with a parasitic element for bandwidth enhancement," *IEEE Antennas and Propagation*, Vol. 53, No. 12, 3930–3939, 2005.

20. Baik, J.-W., T.-H. Lee, S. Pyo, S.-M. Han, J. Jeong, and Y.-S. Kim, "Broadband circularly polarized crossed dipole with parasitic loop resonators and its array," *IEEE Transactions on Antennas and Propagation*, Vol. 59, No. 1, 80–88, 2011.

21. Wong, K. L., J. S. Kuo, and T. W. Chiou, "Compact microstrip antennas with slots loaded in the ground plane," *Eleventh International Conference on Antennas and Propagation*, Vol. 2, 623–626, 2001.